number of 1.1×10^5 is found to be consistent with a backward extrapolation of those data provided in Ref. 5 for Reynolds numbers varying from 3 to 9×10^6.

The marked increase in the lift coefficient with the addition of the rippled trailing edges is directly related to the alleviation of separation in the trailing-edge region at virtually all angles of attack. It is noted that the maximum lift coefficient is increased by approximately 12% (from 0.73 to 0.82) and occurs at an angle of attack 3 deg lower than that of the straight-trailing-edge case.

Drag polars for the two airfoils studied are presented in Fig. 4. These have been normalized with the minimum drag of the basic airfoil in order to isolate wind-tunnel installation effects and allow focus on the relative changes induced by the rippled trailing edge. Here it is seen that the basic airfoil displays a classical drag bucket with a rapid rise in the drag at a lift coefficient of approximately 0.6. The rippled trailing-edge airfoil shows a significantly wider drag bucket than its straight-trailing-edge counterpart. The relative increase in minimum drag for the RTE is expected due to the increase in wetted surface and three-dimensional skewing in the boundary layer. This latter effect is manifest in a spanwise periodic array of axial vortices emanating from the trailing edge as evidenced by complementary flow-visualization studies performed in a water tunnel with the same airfoil. The attendant drag increase for $C_L \leq 0.6$ is not considered of serious consequence because the principal focus here is increase of maximum lift through delay of the separation and stall process. In this regard, the RTE concept in Fig. 4 is seen to achieve this with a resulting significant increase in maximum lift/drag ratio.

Concluding Remarks

The results reported here clearly indicate that through use of controlled lateral-surface contouring, one can provide a mechanism for alleviation of boundary-layer separation effects and thereby produce aerodynamic shapes that yield higher maximum lift and/or lower drag at high lift. The basic separation/alleviation mechanism is the presence of local lateral pressure gradients that are less severe than the normal axial adverse pressure gradient that would otherwise exist in a trailing-edge region. These in turn provide a route for the low-momentum fluid in the surface boundary layer to be scrubbed off into clashing lines and high-momentum inviscid flow brought to the surface. This in turn permits the aerodynamic shape more nearly to achieve its potential flow equivalent lift while generating less drag than its separated-flow counterpart. Further study should now be conducted at high Reynolds numbers in more realistic high-lift situations.

Acknowledgments

This work was conducted as part of the UTRC independent research program. The authors wish to acknowledge the assistance of Mr. Paul Croteau, a former student at Western New England College, in conducting the experimental tests described here.

References

[1]Kimball, S., "Vortex Generators," *Road and Track*, Vol. 36, Jan. 1985, pp. 122–124.

[2]Schubauer, G. B. and Spangenberg, W. G., "Forced Mixing in Boundary Layers," *Journal of Fluid Mechanics*, Vol. 8, May 1960, pp. 10–32.

[3]Grose, R. M., "Theoretical and Experimental Investigations of Various Types of Vortex Generators," United Aircraft Corp., East Hartford, CT, Research Rept. R15362-5, 1954.

[4]Hama, F. R., "An Efficient Tripping Device," *Journal of the Aeronautical Sciences*, Vol. 24, March 1957, pp. 236–237.

[5]Abbott, I. H. and VonDoenhoff, A. E., "Theory of Wing Sections," Dover Publications, New York, 1959.

Pressure Fluctuation Measurements with Passive Shock/Boundary-Layer Control

S. Raghunathan*
The Queen's University of Belfast
Belfast, Northern Ireland

Nomenclature

C_p	= pressure coefficient
C	= model chord length
f	= frequency
H	= tunnel height
$\sqrt{nF(n)}$	= forcing function
M_{S0}	= shock Mach number at zero porosity
n	= frequency parameter fC/U_∞
ps	= porosity open area/model area
$\tilde{p}$	= rms pressure fluctuations
q_∞	= freestream freestream dynamic pressure
t	= thickness of model
U_∞	= freestream velocity
$x_{S0,T}$	= nondimensional shock position transducer position

Introduction

RECENT theoretical and experimental investigations[1-5] have demonstrated that a significant reduction in drag and increase in lift can be obtained in transonic flows with shock waves by the application of passive shock-wave/boundary-layer control (PSBL). The experiments of Theide et al.[4] seem to suggest that PSBL control can also suppress buffeting. However, there has been no attempt, to date, to measure in detail the unsteady aerodynamic excitation of pressure fluctuations in a passively controlled shock/boundary-layer interaction. This Note presents experimental results of pressure fluctuation measurements on a wall-mounted circular-arc half-model in a transonic tunnel with and without PSBL at shock Mach numbers 1.3 and 1.37.

Experiments

Experiments were performed in a blowdown transonic tunnel, 101 mm square with an atmospheric intake. The test section had closed sidewalls and roof, a slotted floor, and 9.6% porosity. The model was a circular-arc half-airfoil of 101-mm chord, 6% thickness, ratio, and 101-mm span, set on the tunnel roof, with the leading edge of the model 560 mm from the beginning of the constant-area test section (Fig. 1). Tunnel blockage $t/H = 6\%$, and effective chord-to-tunnel height $C/H = 0.5$. The recommended values are $t/H < 1.5\%$ and $C/H < 0.4$. However, these are not regarded as critical because the measurements were only of comparative nature. The momentum thickness Reynolds number at the foot of the shock $R = 10^4$. Although mounting a model on the tunnel roof in a small tunnel produced a relative boundary-layer thickness much larger than that encountered in free flight, the resulting momentum thickness Reynolds number at the foot of the shock of $R = 10^4$ was comparable to that which can be obtained by a model mounted in the freestream of larger tunnels. For the porous model, the porous region consisted of 1-mm-diam holes,

Received Dec. 18, 1985; revision received July 18, 1986.

*Senior Lecturer, Department of Aeronautical Engineering. Member AIAA.

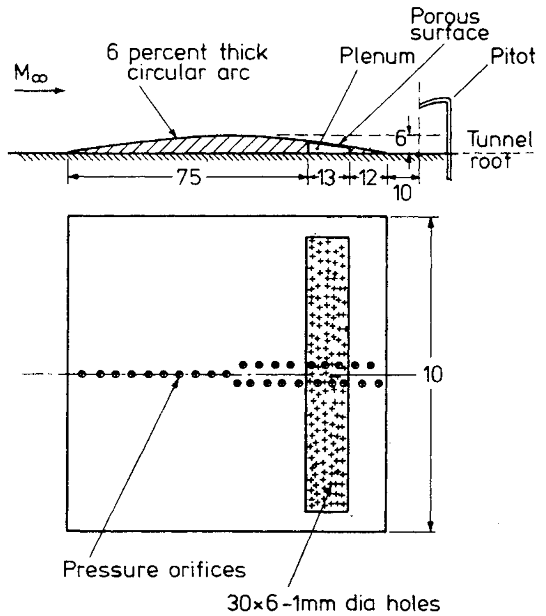

Fig. 1 Circular arc model.

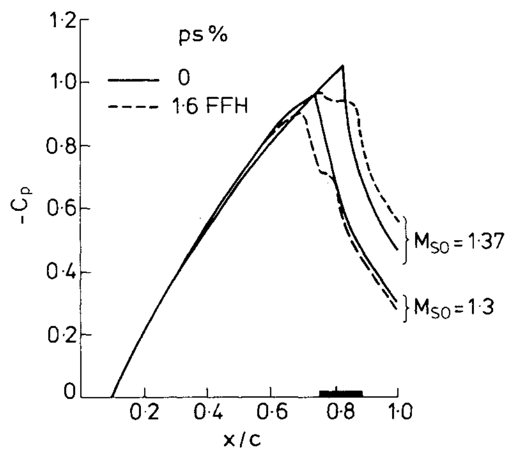

Fig. 2 Pressure distributions.

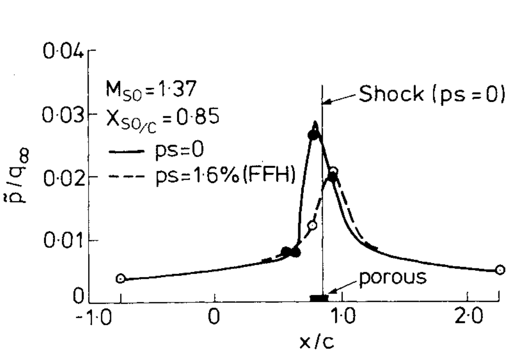

Fig. 3 Pressure fluctuation levels.

forward-facing and inclined at 60 deg to the normal in the region $x/c = 0.75$ to 0.88 with a plenum underneath. The porosity of the model based on the model total surface area was 1.6%. The average plenum depth was 4 mm, resulting in a ratio of the diameter of holes to boundary-layer displacement thickness of approximately 4. The model had four Kulite pressure transducers (type XCS 062) located beneath 1-mm-diam orifices at four positions: $x_T = 0.57$, 0.68, 0.78, and 0.92. The positions of the transducers were offset 2.5 mm from the model centerlines. Earlier pressure measurements have shown that the pressure distribution was virtually constant across an 80% span of the model.

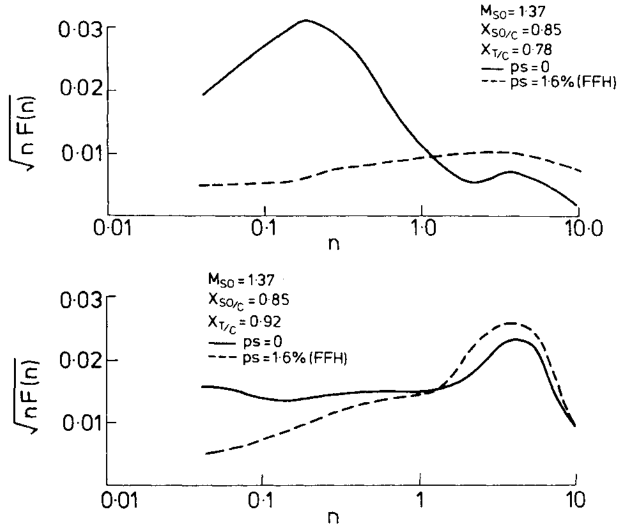

Fig. 4 Spectra of pressure fluctuations.

Experiments were performed at two shock Mach numbers of $M_{S0} = 1.3$ and 1.37, with and without porosity.

Results and Discussions

The pressure distributions for the solid model (SM) are compared with those for the forward-facing holes (FFH) model for the two shock positions of $x_{S0} = 0.75$ and 0.82 ($M_{S0} = 1.3$ and 1.37) in Fig. 2. For the solid model, the trailing-edge divergence of C_p, at both shock Mach numbers, indicate separation of flow downstream of the shock wave. It can be observed that the PSBL control reduces the pressure change across the shock wave. In fact, shadowgraph pictures[3] have shown that the effect of PSBL control is to split a single shock wave into a number of weaker shock waves, resulting in a reduction in the entropy change across the shock system and the drag. It can also be argued that PSBL results in a recirculating airflow in the porous region, which effectively changes the surface geometry and therefore the pressure distribution. The plenum chamber may also act as a communication channel between downstream and upstream regions of the shock wave; therefore, the boundary layer upstream of the shock wave starts thickening as it approaches the shock, which in turn will result in a number of weaker waves, with the shock system spread over a region. This is similar to the situation in a laminar boundary-layer/shock-wave interaction, although the boundary layer is turbulent.

The root-mean-square values of pressure fluctuation levels $\tilde{p}$ nondimensionalized with respect to the freestream dynamic pressure q_∞, based on the sidewall static pressure measurement two chord upstream of the model leading edge, on the model surface and upstream and downstream of it, are shown in Fig. 3. The results shown here are for $M_{S0} = 1.37$, $x_{S0} = 0.85$, and for SM and FFH models. For the SM model, the $\tilde{p}/q_\infty$ values increase to a maximum value at the shock position, but the values are not significantly high (<3%) to indicate any severe shock oscillations. In fact, the distribution of $\tilde{p}/q_\infty$ is typical for a rather steady shock-induced separation. The effect of PSBL is to reduce the $\tilde{p}/q_\infty$ values considerably at the shock position, with a slight increase downstream of it. This suggests that the plenum chamber, which sets up a communication to both sides of the shock wave, acts as a stabilizer for any shock movement. It should be interesting to perform similar investigations in a situation involving strong shock oscillations.

The spectra of pressure fluctuations plotted in the form $\sqrt{nF(n)}$ vs n, where $\sqrt{nF(n)}$ is the forcing function and n

the reduced frequency, are shown in Figs. 4a and 4b for $M_{S0} = 1.37$ and for two transducer positions $x_{T/C} = 0.78$ and 0.92.

The forcing function $F(n)$ is the contribution to $(\tilde{p}/q_\infty)^2$ in the nondimensional frequency band dn such that

$$(\tilde{p}/q_\infty)^2 = \int_{n=0}^{n=\infty} F(n)\mathrm{d}n$$

It is clear from these figures that the effect of PSBL is to reduce the levels at lower frequencies significantly (< 1 KHz) and to increase the levels slightly at higher frequencies. The solid surface model shows a peak in spectra at $n \approx 0.28$ at the shock position. This would correspond to a frequency parameter of $2\pi fc/U_\infty = 1.13$, which compares well with the other experimental values[6] measured at the shock position. The reduction in the pressure fluctuation levels at low frequencies will also reduce the buffeting associated with shock oscillations and shock-induced separation.

Conclusions

It may be concluded from these investigations that PSBL control in transonic flow can reduce pressure fluctuations in the region of shock/boundary-layer interaction and therefore suppress buffeting.

Acknowledgments

The author wishes to acknowledge the financial support given by the Science and Engineering Research Council, U.K. for these investigations. The author also wishes to thank Mr. D.G. Mabey of RAE, Bedford, and Mr. D.J. Butter of the British Aerospace Group, Manchester, for their valuable suggestions.

References

[1]Bahi, L., "Passive Shockwave/Boundary Layer Control for Transonic Super Critical Aerofoil Drag Reduction," Ph.D. Thesis, Rensselear Polytechnic Institute, Troy, NY, 1982.

[2]Nagamatsu, H. T., Dyer, R., and Ficarra, R. V., "Supercritical Airfoil Drag Reduction by Passive Shockwave/Boundary Layer Control in the Mach Number Range 0.75-0.9," AIAA Paper 85-0207, Jan. 1985.

[3]Raghunathan, S. and Mabey, D. G., "Passive Shockwave Boundary-Layer Control Experiments on a Circular Arc Model," AIAA Paper 86-0285, Jan. 1986.

[4]Theide, P., Krogman, P., and Stanewsky, E., "Active and Passive Shockwave/Boundary Layer Control of Supercritical Airfoil," AGARD-FDP Symposium, Brussels, Beligum, May 1984.

[5]Chen, C. L., Chen, Y. C., Holst, T. L., and Van Daisem, W. R., "Numerical Study of Porous Airfoils in Transonic Flow," NASA TM-86713, 1985.

[6]Mabey, D. G., Welsh, B. L., and Cripps, B. E., "Periodic Flows over a Rigid 14% Thick Biconvex Wing at Transonic Speeds," RAE TR-81059, 1981.

Initial Instability in a Freejet Mixing Layer Measured by Laser Doppler Anemometry

S. Einav,* J. M. Avidor,* and E. Gutmark*
Tel Aviv University, Israel
and
M. Gaster†
National Maritime Institute, Teddington, England

I. Introduction

MUCH attention has been focused in recent years on the instability waves that develop at the origin of free turbulent shear layer. Michalke[1] calculated the spatial growth of small perturbation in a shear layer with a finite thickness. He found that the most amplified instability frequency f_0 can be scaled with the initial momentum thickness Θ_0 and the jet exit velocity V_0. The Strouhal number based on this scaling was a constant:

$$St_0 = f_0 \frac{\Theta_0}{V_0} = 0.017$$

Many investigators confirmed[2-4] these calculations, the values varying from 0.01 to 0.018. The jet's initial momentum thickness varies with the exit velocity as $V_0^{-1/2}$. Hence, f_0 should be proportional to $V_0^{3/2}$. Contrary to this prediction, Gutmark and Ho[5] observed a stepwise variation of the initial instability frequency with the jet velocity, in several facilities. A possible cause for this discrepancy was interference by the hot-wire probe. Hussain and Zaman[6] have shown that when a probe is placed in the shear layer, it can trigger, by its presence, flow instabilities that have characteristics similar to those observed in the above-mentioned experiments. The purpose of the present study was to rule on this possibility by initializing a nonintrusive technique, namely, laser Doppler anemometry (LDA). This technique was used to measure the behavior of the initial instability of the jet, and the results were compared with those obtained by using the conventional hot-wire anemometer on the same system. In this study, velocity spectra were generated from the LDA velocity measurements with the aid of a spectral technique outlined in Sec. III. The results of the present work showed identical behavior of the initial instability frequency as reported by Gutmark and Ho.[5]

II. Facility and Instrumentation

The measurements reported in this paper were performed in an axisymmetric jet operating from a compressed air supply. A contraction section with a fifth-order polynomial profile and contraction ratio of 64 led from the stagnation chamber to a nozzle with a diameter D of 25.4 mm. Honeycombs and layers of fine screen were used to reduce the turbulence intensity. As a result, the turbulence level was less than 0.4% in the operating velocity range.

The laser Doppler anemometer, depicted in Fig. 1, is based on a dual-beam system operating in the forward scattering mode.[7] A continuous-wave (CW) argon-ion laser emitting 1.5 watts at 514.5 nm has been employed as the light source for the LDA. In order to obtain spectra with a few kHz bandwidth, one has to resort to artificial seeding of the jet flow. In this experiment the aerosol was generated with a Laskin nozzle and limited to small particles by a one-stage cascade impactor. The artificially generated aerosol was injected in the plenum of the jet.

LDA signal processing was carried out in the following way: The photomultiplier output was amplified, filtered, and processed by the Thermo Systmes Inc. burst counter. Using a minicomputer, these data were stored in files, each containing a string of Doppler frequencies and the respective time interval

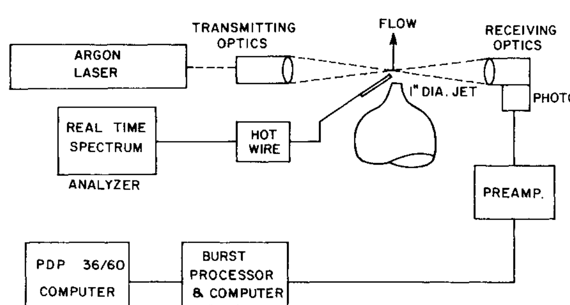

Fig. 1 Laser Doppler anemometer system.

Received July 6, 1985; revision received Jan. 1, 1986.

*Faculty of Engineering, Department of Fluid Mechanics.

†Senior Principal Scientific Officer, Applied Fluid Mechanics.